Neumann boundary condition for the stream function, a point-image and the steady-state stream function equation evaluated at the wall.

It is noteworthy that the proposed approach is applicable to any set of time-discretized systems of partial differential equations. Moreover, it is extremely simple since it does not require that any "logical choices" be made or "free parameters" be tuned and it does not need any additional storage with respect to the basic smoother (insofar as only the finest-grid solution is computed and a single array is used for the deltas at all grid levels). However, its work per iteration is slightly greater than that required by most current multigrid methods, additional interpolations and collections being needed to visit and update the finest-grid solution after every coarse-grid calculation. Also, no convergence theorem exists for this method, so that numerical experiments are required to assess its merits.

III. Results

The proposed methodology has been applied to solve three different sets of equations, namely, the Laplace equation, the vorticity-stream function Navier-Stokes equations (for the case of the classical driven cavity flow at $Re = 1000$), and the lambda-formulation Euler equations (for the case of a two-dimensional subsonic source-flow). For the first, simple problem, the method possesses a typical multigrid convergence rate that is practically independent of the size of the finest grid used in the computation (see Ref. 8 for details). For the second, reasonably difficult problem, the method, as previously described, was applied starting from rest, using a nonoptimized unitary time step for both equations, an overrelaxation factor $\alpha = 1.5$, and the standard 9-point collection operator for the residual. The convergence history of the method, using a 65×65 uniform finest mesh and from one to four grid levels, is given in Fig. 1 as the average residual of the vorticity equation versus the work units. The improvement provided by the proposed multigrid approach is quite clear—machine zero (using single precision arithmetic on an HP 9000/9050 minicomputer) is obtained after almost 1500 work units (iterations) using the single grid smoother and after only about 200 work units using four grid levels. It appears quite remarkable, indeed, that such a naive method not only improves the asymptotic convergence rate significantly but also reduces the length of the plateau in the convergence history. It may be of interest to know that the work units per iteration, for the present calculation, are equal to 1.49, 1.88, and 2.26 for the case of two, three, and four grids, respectively (one work unit requires about 8 CPU seconds on the aforementioned minicomputer).

The proposed approach was finally applied to solve the lambda-formulation Euler equations in two dimensions for the case of a subsonic source flow. For such a case, an explicit one-step method was used as smoother, simple injection was used also for the RHS residual and the time step, limited by the CFL condition, was doubled on each coarser-mesh computation. The convergence rate is given in Fig. 2 as the average residual of the three governing equations versus the work units. The validity of the proposed multigrid strategy is again quite clear. It is noteworthy that machine zero is reached at a higher value of the residual (which is proportional to the computed deltas divided by the time step) and is due to the small time step used in the calculations. For the present computations, using an explicit smoother and simple injection for the residuals, the work units per step are equal to 1.47, 1.82, and 2.16 for the case of two, three, and four grid levels, respectively (one work unit requires about 2 CPU seconds).

IV. Conclusions and Future Work

A novel incremental multigrid strategy has been proposed to solve the equations of fluid dynamics. It provides considerable efficiency gains for the case of elliptic, mixed parabolic-elliptic, and hyperbolic problems. With respect to current well-established multigrid schemes, the proposed approach is algorithmically simpler but requires more work per iteration and, at present, has been shown to be effective only for subsonic flow problems and uniform grids. Current work is attempting to remove both limitations and to demonstrate the applicability of the method to the very important case of the compressible Navier-Stokes equations in conservation-law form.

Acknowledgments

This work was supported by Consiglio Nazionale Ricerche, Ministero Pubblica Istruzione, and by ONR Grant N00014-82-K-0184 while the author was in residence at Yale University's Research Center for Scientific Computation. The author is indebted to Drs. W. J. Usab Jr. and R. L. Davis for many helpful suggestions and stimulating discussions, to Dr. M. J. Werle for making their cooperation possible, and to Professor L. Quartapelle for revising this manuscript.

References

[1] Dadone, A. and Napolitano, M., "An Implicit Lambda Scheme," *AIAA Journal*, Vol. 21, Oct. 1983, pp. 1391-1399.

[2] Dadone, A. and Napolitano, M., "An Efficient ADI Lambda Formulation," *Computers and Fluids*, Vol. 13, No. 4, 1985, pp. 383-395.

[3] Napolitano, M., "Efficient ADI and Spline ADI Methods for the Steady-State Navier-Stokes Equations," *International Journal for Numerical Methods in Fluids*, Vol. 4, 1984, pp. 1101-1115.

[4] Napolitano, M. and Walters, R. W., "An Incremental Block-Line-Gauss-Seidal Method for the Navier-Stokes Equations," *AIAA Journal*, Vol. 24, May 1986, pp. 770-776.

[5] Beam, R. M. and Warming, R. F., "An Implicit Factored Scheme for the Compressible Navier-Stokes Equations," *AIAA Journal*, Vol. 16, April 1978, pp. 393-402.

[6] Isaacson, E. and Keller, H. B., *Analysis of Numerical Methods*, John Wiley & Sons, Inc., New York, 1966.

[7] Khosla, P. K. and Rubin, S. G., "A Diagonally Dominant Second-Order-Accurate Implicit Scheme," *Computers and Fluids*, Vol. 2, 1974, pp. 207-209.

[8] Napolitano, M., "An Incremental Multigrid Strategy for the Fluid Dynamic Equations," *Proceedings of the AIAA Seventh Computational Fluid Dynamics Conference*, 1985, pp. 269-274.

Wavy Wall Solutions of the Euler Equations

Philip Beauchamp*
General Electric Company, Lynn, Massachusetts
and
Earll M. Murman†
Massachusetts Institute of Technology
Cambridge, Massachusetts

Introduction

THE steady inviscid irrotational flow of a compressible fluid past a small amplitude sinusoidally varying wavy wall has been well explained using small perturbation theory.[1] For subsonic and supersonic flow, the solutions are analytically obtained by neglecting higher order terms in the pertur-

Received March 8, 1986; revision received May 22, 1986.

*Technical Engineer. Member AIAA.

†Professor, Aeronautics and Astronautics. Associate Fellow AIAA.

bation equations. For transonic and hypersonic flow, the small perturbation equations contain additional nonlinear terms which may not be neglected. Consequently, the equations must be solved numerically. Chang and Kwon[2] have performed numerical calculations in the nonlinear region corresponding to transonic flow.

The solutions to the wavy wall problem that were obtained using the classic approximations are, as a consequence of Crocco's relation, isentropic. The validity of using this model to compute a transonic flow with shocks must be questioned. The transonic casses studied by Chang and Kwon result in shocks that would cause a total pressure loss of almost 0.4%. Consequently, the isentropic flow assumption may be satisfactory for these cases. However, for flows with stronger shocks, the Euler equations would clearly provide a better model of the flow nonlinearities. The use of the Euler equations, however, introduces other issues.

For larger amplitude wavy walls and higher flow velocities, the shock strength may increase dramatically. The resulting entropy increase and total pressure loss would then be convected downstream. Any subsequent shocks would therefore be weakened by the aggregate total pressure loss of the preceding shock(s). Since this flow must have an initial shock followed by a series of weaker shocks, the implication is that the problem may no longer be a boundary value problem but rather an initial value problem. Eventually the flowfield may reach a condition where it is periodic in space; however, there is no guarantee that this is true.

The problem of interest is the time-accurate computation of an inviscid compressible flow past a sinusoidally varying wall of arbitrary amplitude. The Euler equations must be solved numerically. Solutions have been obtained by using two different formulations for the boundary conditions. In the first formulation, the domain consists of a series of sinusoidally varying bumps with a flat wall upstream of the first bump and downstream of the last. In the second formulation, a single wave is examined by imposing periodicity in the flow direction and computing the flow in a time-accurate manner. (A more complete description of this investigation is given in Ref. 3).

Numerical Technique

Determination of the flowfield using the Euler equations requires the development of a discrete approximation to the governing equations. The discretized system must then be integrated in time to determine the solution. In this work, the finite volume multistage scheme developed by Jameson, Schmidt, and Turkel[4] has been used. To reduce the occurrence of odd-even decoupling, a fourth difference smoothing operator is applied to each cell. In addition, a second difference smoothing operator is used to properly capture the shocks. At the boundaries of the domain, the dissipation scheme is modified to maintain global conservation. Following the example of Eriksson,[5] the dissipation flux on each

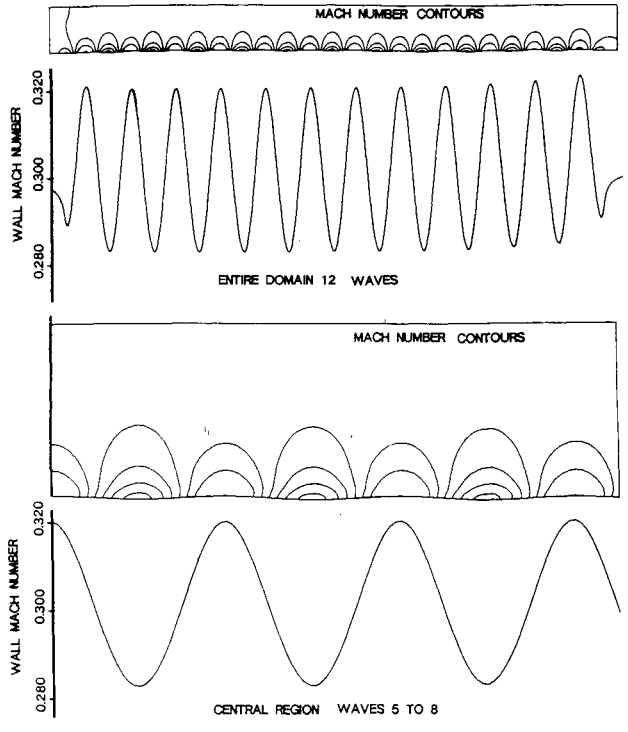

Fig. 1 Subsonic solution over 12 waves, $M_\infty = 0.3$, $\epsilon = 0.01$.

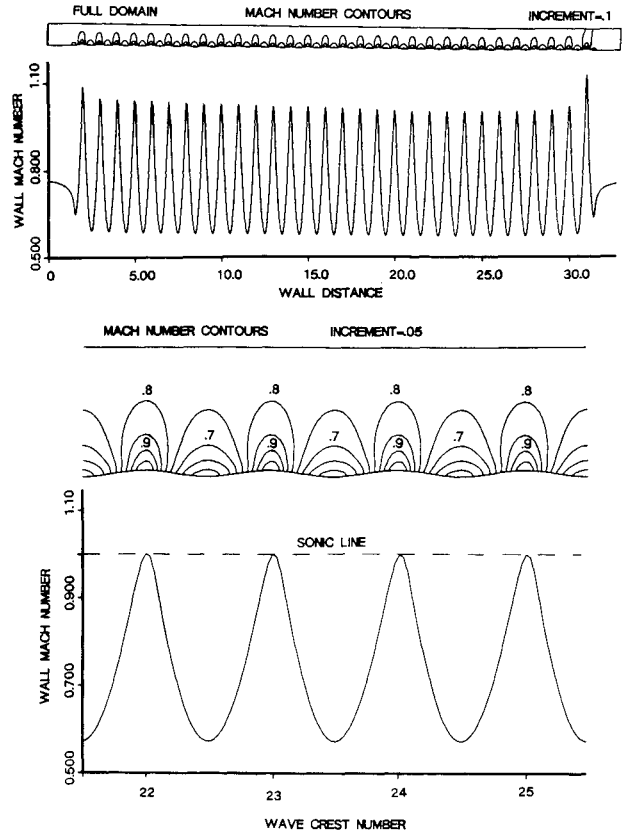

Fig. 2 Transonic solution over 30 waves, $M_\infty = 0.775$, $\epsilon = 0.025$.

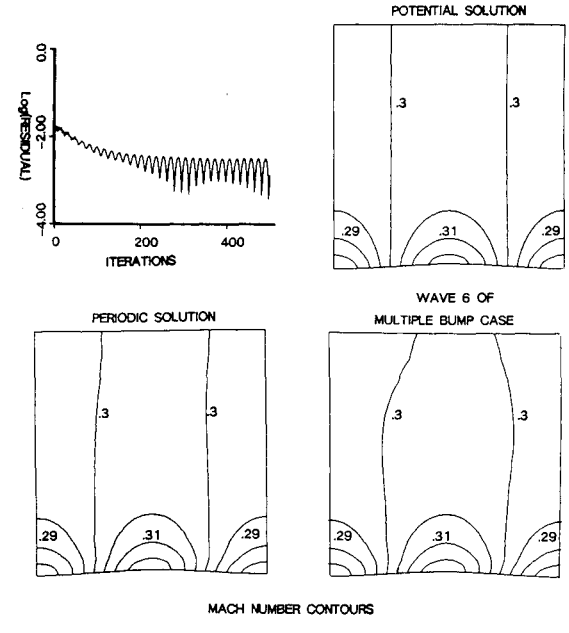

Fig. 3 Subsonic solution using periodic boundaries, $M_\infty = 0.3$, $\epsilon = 0.01$.

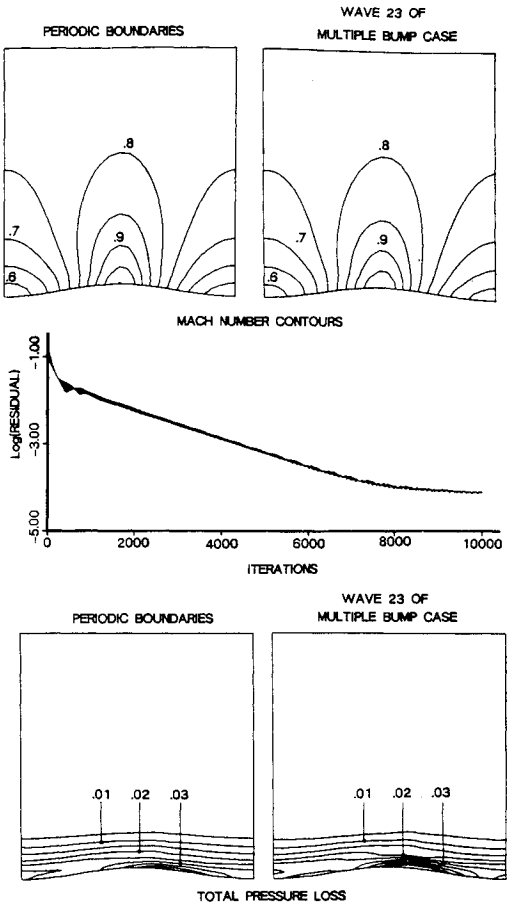

Fig. 4 Transonic solution using periodic boundaries, $M_\infty = 0.775$, $\epsilon = 0.025$.

boundary face is set to zero. The dependence of the solutions on damping parameters was investigated by computational experiments. In agreement with many published results, no significant effects were noted.

In addition to the usual solid wall boundary condition, two other boundary conditions have been used. For the flows using more than one bump, the left, right, and top boundaries are free. For these free regions, a straightforward Riemann invariant[3] boundary condition has been imposed. For the single wave formulation, the left and right faces are assumed to be periodic while the top boundary uses the Riemann invariant formulation.

Time integration is performed using a four-stage Runge-Kutta technique. For the periodic solutions, the integration is performed using a fixed Δt at each cell. The chosen Δt is governed by the Δt for the most restrictive cell in the domain. This leads to rather lengthy computation times, but it is unavoidable for time-accurate solutions using an explicit method. For the multiple bump formulation, only the steady state solution is desired. In this case the integration has been performed using the maximum allowable time step at each cell.

A uniform freestream was used as part of the initial conditions for all solutions presented. In addition, for the periodic boundary problem, the small perturbation potential solution was used for initial conditions. No significant differences were noted in the results.

Multiple Bump Results

Since there is no guarantee that the Euler flow past a wavy wall is periodic in space, a series of multiple bump solutions were attempted for subsonic and transonic conditions. The subsonic flow problem consists of a Mach 0.3 flow over a 0.01 amplitude wave. The transonic solutions are obtained for a Mach 0.775 flow past a 0.025 amplitude wave. For these solutions, the multiple bump region was preceded and followed by a flat wall section of 1.5 wavelengths. All the computations are performed using the Riemann boundary conditions, with the far-field values corresponding to a uniform freestream flow. The objective of these computer intensive computations was to determine if the flows were periodic in space and, if so, over what region of the domain.

Figure 1 illustrates the results obtained for the $M_\infty = 0.3$ subsonic wavy wall. The computation is performed for 12 waves with a 30×20 mesh for each wavelength for a total of 9000 cells. The computation demonstrates that for subsonic flow, the solution is periodic over a wide range of the computational domain. Observe that the flow is not periodic over the first or last two waves of this solution. This is to be expected since the flow is responding to the influence of the adjacent flat wall region for these waves. In addition, the solution in the central region shows a good comparison to the potential solution for the same case.

Figure 2 illustrates the results obtained for the transonic computation. This computation is performed on a 19,800-cell grid for a domain consisting of 30 waves. The solution shows that initially the flow is not periodic. The first wave has a weak shock which generates some small total pressure loss. Succeeding wave crests also have shocks which become successively weaker and consequently generate less and less additional pressure loss. This decaying of the shocks and incrementing of total pressure loss continues until about the 22nd wave crest after which the flow at each wave crest is just sonic. Aft of wave crest 22, as illustrated by the expanded view of wave crests 22-25, the flow appears to be periodic in space. Over the first twenty-two waves the solution has acquired an aggregate total pressure loss of about 3%. Again, the influence of the downstream flat wall can be seen on the last two waves.

Periodic Boundary Results

The solution for the subsonic wavy wall with periodicity imposed between the left and right boundaries is shown in Fig. 3. This figure shows the convergence history and compares the Mach number contours obtained with those of the small perturbation solution and the multiple wave solution. Based on the results of the multiple bump solution, this solution has been iterated a sufficient number of times to allow the flow to be convected through the domain at least three times. Observe that all solutions compare quite favorably.

For transonic flow along a wavy wall, the solution has been obtained by imposing periodicity in the flow direction while allowing the upper boundary to be a Riemann freestream far-field boundary. Figure 4 illustrates the convergence history and compares the Mach number and total pressure loss contours with those obtained for the multiple bump solution. The comparison of the two solutions is very good.

For this case, an entropy layer is created by the shock wave that occurs during the startup process. The entropy rise is convected out of and back into the domain until the shock weakens and disappears. The startup transient is analogous to the initial wave crests of the multiple bump results.

Conclusions

The solutions presented are for the subsonic and transonic flows past a wavy wall. The results of the numerical evaluations of the subsonic wavy wall problem show that the Euler flows appear to be periodic and compare quite well to the classic small perturbation solution. The transonic results show that the solution consists of a series of shocks that become progressively weaker as the fluid flows over each successive wave crest. The weakening process continues until the flow reaches a condition where the stagnation pressure loss is sufficiently high to result in waves with a single sonic point. From this point on the solution appears to be periodic in space. It is reasonable to expect that this behavior would occur over a range of Mach numbers. However, the size and strength of the entropy layer might depend on the path taken to reach steady

state, although this was not noted in the reported results. Solution for the supersonic problem have been attempted.[3] Periodic solutions were not obtained, except for conditions with very weak shocks, as would be expected.

References

[1]Liepman, H. W. and Roshko, A., *Elements of Gasdynamics*, John Wiley & Sons Inc., New York, 1957.

[2]Chang, K. and Kwon, O. J., "Mixed Transonic Flow over a Wavy Wall with Embedded Shock Waves," *Trans. Jap. Soc. Aero. & Space Sciences*, Vol. 25, No. 70, 1983, pp. 189-202.

[3]Beauchamp, P. P., "Euler Solutions to the Wavy Wall Problem," Massachusetts Institute of Technology, Rept. CFDL-TR-86-3, Jan. 1986.

[4]Jameson, A., Schmidt, W., and Turkel, E., "Numerical Solution of the Euler Equations by Finite Volume Methods Using Runge-Kutta Time-Stepping Schemes," AIAA Paper 81-1259, June 1981.

[5]Eriksson, L. E., "Boundary Conditions for Artificial Dissipation Operators," Aeronautical Research Institute of Sweden, FFA TN 1984-53, Oct. 1984.

Theoretical Gain Optimization in CO_2-N_2-H_2 Gasdynamic Lasers with Two-Dimensional Wedge Nozzles

N. M. Reddy,* K. P. J. Reddy,† and M. R. Krishna Prasad‡
Indian Institute of Science, Bangalore, India

Introduction

In an earlier publication,[1] we reported the theoretical gain optimiation studies of a 16-μm CO_2-N_2-H_2 gasdynamic laser (GDL) in which it was showed that the optimum value of a 2.06% cm^{-1} gain could be obtained with conical or hyperbolic nozzles. In this Note, we report the results of optimization studies with a 16-μm CO_2-N_2-H_2 GDL using two-dimensional wedge nozzles. We have found that the optimum value of the gain that can be achieved is as high as 12.7% cm^{-1} on the P(15) line of the $(02^00)\rightarrow(01^10)$ transition of CO_2 for a gas mixture composition of CO_2:N_2:H_2 = 30:50:20%. The corresponding optimum values for the reservoir pressure and area ratio are computed as functions of the resevoir temperature and presented graphically. Results are presented for a range of gas mixture compositions.

Governing Equations

The global mass, momentum, and energy conservation equations governing the steady inviscid quasi-one-dimensional flow of a CO_2-N_2-H_2 gas mixture in a supersonic nozzle of a GDL are considered along with the equation of state. Equations governing the vibrational energy exchange through bimolecular collisions are also considered. Two additional algebraic equations for the population inversion (PI) and the small-signal optical gain (G_0) are obtained as functions of the flow quantities from the basic governing equations. All of these equations (which are in dimensional form) are normalized with respect to a chosen set of reference values and then reduced to universal form by suitable transformation of the independent variable, so that the solutions depend on a single universal parameter χ_I that combines all of the other parameters in the system. The governing equations and the equations for PI and G_0 in their final form are given in Ref. 1.

Received Aug. 16, 1985; revision received April 17, 1986.

*Professor, Department of Aerospace Engineering.
†Senior Scientific Officer, Department of Aerospace Engineering.
‡Scientific Assistant, Department of Aerospace Engineering.

The following functions are used for solving the equations in the present case.

1) The nonsimilar function:

$$\begin{aligned} N_s &= 0.0, && \text{for } (\xi_*/\xi) < 0.980 \\ &= 0.03 - 12.5(0.990 - \xi_*/\xi)^{1.208} && \text{for } 0.980 \le (\xi_*/\xi) < 0.990 \\ &= 0.2747 - 1.676\times 10^{-2}(\xi_*/\xi - 0.96)^{-0.85} && \text{for } (\xi_*/\xi) \ge 0.990 \end{aligned} \tag{1}$$

where ξ is an independent parameter.

2) The mass flow factor ($\rho_* u_*$) and the density ρ_*:

$$\rho_* u_* = 0.669 = \text{const} = K_1 \tag{2}$$

$$\rho_* = 0.6338 = \text{const} = K_2 \tag{3}$$

3) The normalized velocity ratio (u/u_*):

$$\begin{aligned} (u/u_*)K_1^{8.08} &= -0.0036 + 0.0635(0.650 + \log_{10}A)^{-3.176} && \text{for } M < 1.0 \\ &= 0.5937 - 0.13789(0.250086 + \log_{10}A)^{-0.7194} && \text{for } M \ge 1.0 \end{aligned} \tag{4}$$

where A is the normalized area ratio, M the Mach number, and subscript (*) the throat conditions.

Results

Following the numerical scheme given in Ref. 2, the governing equations are solved for the normalized values of the translational temperature ψ and the vibrational temperatures ϕ_I and ϕ_{II} of modes I and II, respectively, for a family of wedge nozzles ($ij = 1.0$) with χ_I as a parameter. Computations are carried out for a range of mixture compositions, for a H_2 mole fraction having a 5-20% variation with a CO_2 mole fraction variation of 2.5-30% for each H_2 mole fraction. Variations in ψ, ϕ_I, and ϕ_{II} along the nozzle are computed for each case and used to compute the corresponding values of PI and G_0.

A typial variation of these solutions for a sample case of CO_2:N_2:H_2 = 20:73:7% are presented in Fig. 1, where gain G_0 attains a maximum, while the PI remains constant far downstream of the throat. Such peak values for G_0 are computed for a range of mixture compositions and over a range of χ_I values for each composition. The plots of maximum values of G_0 vs χ_I are shown in Fig. 2 for different CO_2-N_2 concentrations with 20% of H_2 mole fraction. This particular set is presented because the optimum gain shown is the highest in the wide range of mixture compositions for which the optimum gain values are computed. From these graphs, it is clear that, for every gas mixture, G_0 attains a maximum, designated as $(G_0)_{opt}$, at a particular value of χ_I, designated as $(\chi'_I)_{opt}$ and representing the optimum value. Thus, for a given laser gas mixture composition, $(G_0)_{opt}$ represents the highest possible value of small-signal gain that can be achieved. For example, the $(G_0)_{opt}$ equal to 12.7% cm^{-1} occurs at a $(\chi_I)_{opt}$ value of 2.5 for a gas mixture composition of CO_2:N_2:H_2 = 30:50:20% as shown in Fig. 2. The variation of $(G_0)_{opt}$ is shown in Fig. 3 for various CO_2 and H_2 concentrations.

Optimum operating conditions, such as the reservoir temperature and pressure corresponding to the optimum value of G_0 for any given laser mixture, can be readily calculated using the corresponding $(\chi_I)_{opt}$ value. Since the universal parameter χ_I is a function of the reservoir temperature T_0' and